



HAL
open science

Chalcogen Bonding with Diaryl Ditellurides: Evidence from Solid State and Solution Studies.

Robin Weiss, Emmanuel Aubert, Loic Gros Lambert, Patrick Pale, Victor Mamane

► **To cite this version:**

Robin Weiss, Emmanuel Aubert, Loic Gros Lambert, Patrick Pale, Victor Mamane. Chalcogen Bonding with Diaryl Ditellurides: Evidence from Solid State and Solution Studies.. Chemistry - A European Journal, In press, 10.1002/chem.202200395 . hal-03615217

HAL Id: hal-03615217

<https://hal.science/hal-03615217>

Submitted on 30 Mar 2022

HAL is a multi-disciplinary open access archive for the deposit and dissemination of scientific research documents, whether they are published or not. The documents may come from teaching and research institutions in France or abroad, or from public or private research centers.

L'archive ouverte pluridisciplinaire **HAL**, est destinée au dépôt et à la diffusion de documents scientifiques de niveau recherche, publiés ou non, émanant des établissements d'enseignement et de recherche français ou étrangers, des laboratoires publics ou privés.

Chalcogen Bonding with Diaryl Ditellurides: Evidence from Solid State and Solution Studies.

Robin Weiss,^[a] Emmanuel Aubert,^[b] Loic Gros Lambert,^[a] Patrick Pale^{*,[a]} and Victor Mamane,^{*,[a]}

[a] Dr. R. Weiss, L. Gros Lambert, Prof. Dr. P. Pale, Dr. V. Mamane
Institute of Chemistry of Strasbourg, UMR 7177 - LASYRO
CNRS and Strasbourg University
4 rue Blaise Pascal, 67000 Strasbourg, France
E-mail: vmamane@unistra.fr (VM); ppale@unistra.fr (PP)
Twitter: @mamane_victor

[b] Dr. E. Aubert
Université de Lorraine, CNRS, CRM2, F-54000 Nancy, France

Abstract: The chalcogen bonding (ChB) ability of Te is studied in symmetrical diaryl ditellurides ArTeTeAr. Among the two Te σ -holes, the one along the less polarized Te-Te bond was calculated as the more electropositive. This counter-intuitive situation is due to the hyperconjugation contribution from Te lone pair to the σ^* of the adjacent Te which coincides with σ -hole along the more polarized Te-Ar bond. ArTeTeAr showed notable structural features in the solid state as a result of intermolecular Te...Te ChB, such as a Te₄ rectangle through dimer aggregation or a triangular Te₃ motif, where one Te interacts with both Te atoms of a neighboring molecule through both its σ -hole and lone pair, in a slightly frustrated geometry. Lewis acidity of ArTeTeAr was also evaluated by NMR with R₃PO as σ -hole acceptors in different solvents. Thus, ¹²⁵Te NMR allowed monitoring Te...O interaction and delivering association constants (K_a) for 1:1 adducts. The highest value of $K_a = 90 \text{ M}^{-1}$ was measured for the adduct between ArTeTeAr bearing CF₃ groups and Et₃PO in cyclohexane. Notably, by using *n*Bu₃PO, Te...O interaction was revealed by ¹⁹F-¹H HOESY showing spatial proximity between CF₃ and CH₃ of *n*Bu₃PO.

Introduction

Non-covalent interactions based on σ -hole have gained increasing interest in chemistry since the beginning of the 21st century. The halogen bond (XB) is the archetype of such interaction, identified and then exploited in diverse areas such as organocatalysis,^[1] medicinal chemistry^[2] and crystal engineering,^[3] to name a few. Together with earlier observations showing that chalcogen–chalcogen interactions are driving forces for the formation of superstructures in crystals of chalcogen-rich organic compounds,^[4] the XB reports have stimulated new studies concerning similar noncovalent interactions centered on other elements such as chalcogens (S, Se, Te).^[5] This led to term such interactions as chalcogen bond (ChB) in analogy to XB, and to recently define them as *a net attractive interaction between an electrophilic region associated with a chalcogen atom in a molecular entity and a nucleophilic region in another, or the same, molecular entity.*^[6] This electrophilic region, called σ -hole (blue area in Figure 1A), is located at the antipode of the Ch-R bond and spatially coincides with the LUMO orbital (σ^*) of the Ch-R bond. Because of their divalent character, each chalcogen atoms possess two σ -holes (Figure 1A).^[7] As for XB, ChB strength depends on the polarizability of the chalcogen atom (S < Se < Te). Indeed, crystal structures and calculations revealed that within chalcogen interactions, the tellurium–chalcogen ones are the strongest, particularly if an electron-withdrawing group is attached to the tellurium center.^[8]

Tellurium derivatives are thus becoming the most promising for applications based on σ -hole interactions, with a few emerging in anion recognition^[9] and binding^[10] and in catalysis.^[11] Nevertheless, applications remain scarce, probably due to the lack of data on these interactions, especially in solution. A better understanding of these interactions would obviously lead to further applications.

Based on such considerations, we are thus conducting detailed investigations of selected organotellurium compounds in order to tune σ -hole deepness and look at the resulting interactions^[12], in the solid state but mostly in solution, with the aim to apply them to catalysis.^[11e] For the present study, we selected diaryl ditellurides where each tellurium atom possesses two σ -holes at the antipode of C-Te ($\sigma_{\text{Te-C}}$) and Te-Te ($\sigma_{\text{Te-Te}}$) bonds (Figure 1B). These two σ -holes are expected to have inherently different strengths which should strongly influence their solid-state and solution properties.

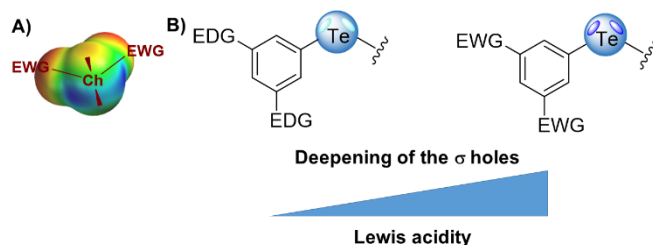
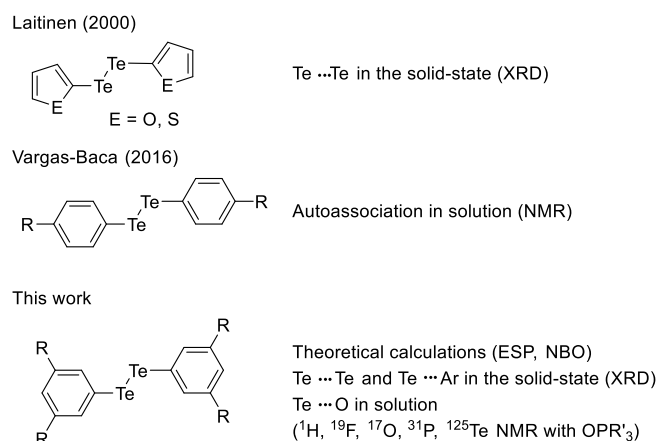


Figure 1. A) Location of chalcogen σ -holes (colors towards red depict negative values while colors towards blue depict positive values, and colors in between (orange, yellow, green) depict intermediate values). B) Lewis acidity in organotellurium compounds. The enhancement of the blue color represents a greater positive electrostatic potential surface on the Te σ -hole. EDG = Electron Donating Group; EWG = Electron Withdrawing Group.

Far less studied than their monotelluride counterparts,^[8,13] ditellurides are nevertheless known to exhibit peculiar properties, that can now be understood as the results of σ -hole interactions. Diaryl ditellurides present chiroptical properties in the solid state, due to their skewed conformation which induces helicity.^[14] Their crystal structures revealed short intermolecular Te...Te contacts,^[15] clearly resulting from ChB in which Te is acting both as ChB donor and acceptor. Evidences of auto-association of diaryl ditellurides have also been reported in several solvents.^[16] However, the weakness of these noncovalent interactions seems to have precluded further investigations (Scheme 1). Furthermore, ditellurides exhibit interesting biological properties,^[17] mostly peroxidase-like catalytic activity.^[18] They indeed mimic the action of the selenium-containing glutathione-peroxidases, with 4,4'-substituted diphenylditellurides three to nine times more active than ebselen,^[19] the first agent for hydroperoxide-inactivating therapy.^[20] However, the exact mode of action seems to be still unknown, but could rely on σ -hole interactions.^[21,22]



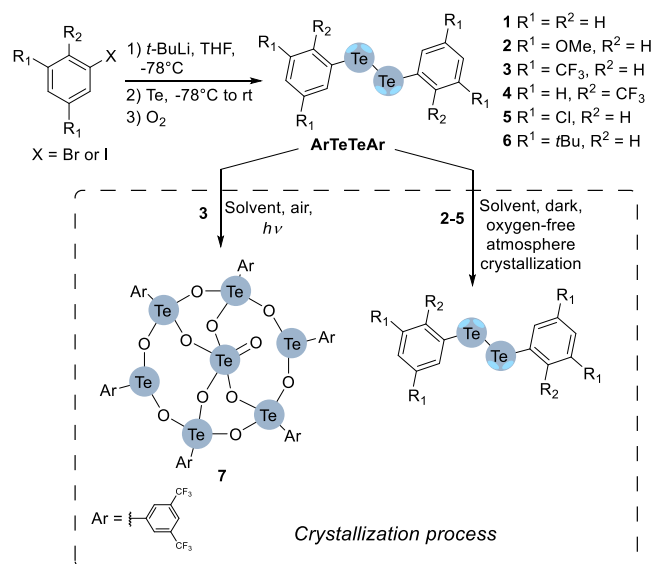
Scheme 1. Previous studies indicating Te...Te interactions and our comprehensive work.

These aspects motivated us to tackle σ -hole interactions involving diaryl ditellurides. More precisely, our aims were to check if the same or similar ChB could occur with such compounds in solution compared to solid state, and if their strengths could be adjusted either by tuning their structures or the condition in solution, and if these strengths could be evaluated. To implement these goals, we reported here the synthesis of different diaryl ditellurides carrying

substituents chosen as electron-withdrawing or -donating groups (EWGs or EDGs). The latter were selected in order to tune the tellurium σ -holes through electronic effects and to induce stronger interactions (Figure 1B). The molecular surface maxima corresponding to both tellurium σ -holes were calculated and their relative values were discussed on the basis on Natural Bond Orbital (NBO) analysis. The ability of diaryl ditellurides to establish ChBs was then evaluated in the solid state by single crystal X-ray diffraction (XRD) and in solution through a combination of NMR techniques, such as ^{125}Te , ^{17}O , ^{31}P NMR, titration and 2D ^{19}F - ^1H HOESY experiments.

Results and Discussion

The known diphenyl ditelluride **1** and the related new ditellurides **2-6** were synthesized from the corresponding aryl halides through halogen-lithium exchange in the presence of *t*-butyllithium followed by addition of grey tellurium at low temperature.^[23] Reactions occurred smoothly to produce red-orange products in good yields (76% to 84%) (Scheme 2). A particular care was taken to exclude oxygen and light as much as possible during the work-up. Without these precautionary conditions, the ditellurides tend to promptly react to form white solid which separate from the solution over the time.^[24] Similar observations have already been reported, but side-products were not conclusively identified, although infrared spectroscopy and elemental analysis suggested the presence of a variety of oxygen-containing species ($\text{R}_2\text{Te}_2\text{O}$, $\text{R}_2\text{Te}_2\text{O}_2$ and $\text{R}_2\text{Te}_2\text{O}_3$).^[16] In our hands, a white powder was obtained in a crystallization attempt of compound **3**, in the presence of light and oxygen. High-resolution mass spectrometry and XRD analysis indicated the presence of **7**^[25] (Figure S1) as a heptanuclear organotellurium oxide cluster whose structure could be analogous to the one reported by R. J. Butcher *et al.*^[26] (Scheme 2). Taken up in DMSO, **7** exhibited broad signals in ^1H NMR spectrum, which could be attributed to slow dynamic exchange because of the large flexibility of the molecular structure of **7**.

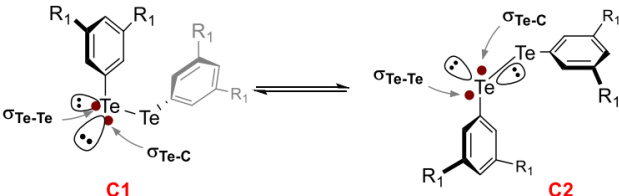


Scheme 2. Diaryl ditellurides synthesis and crystallizations

Among the compounds obtained, **2-5** were successfully crystallized from acetone in the dark by slow evaporation. Their structures were determined by single crystal XRD (Figure S2) and the structural parameters are listed in Tables S1 and S2. **2** and **4** exhibit the less common conformation among the few known ditellurides, with both aryl moieties almost coplanar (see CSD database analysis in SI, §2.4), while **3** and **5** exhibit the most common conformation, with the two aryl groups perpendicular.

To better understand these structures and their conformations and interactions, the anisotropy and magnitude of the electrostatic potential at tellurium centers were characterized by ESP analysis. For this purpose, the geometry of compounds **1-6** was optimized using density functional theory (DFT) with the B3LYP functional (completed with D3 dispersion corrections)^[27] and the Def2TZVPP basis set. For the two most stable conformations **C1** and **C2** (see Scheme of Table 1), the electrostatic potential values (V) were calculated on $\rho=0.001$ a.u. molecular surfaces with the extrema ($V_{s,max}$ and $V_{s,min}$) located using MWFN software^[28] (Figures S42-S51) and reported in Table 1. For compounds **2-5**, the V_{max} values of optimized geometries were compared with those calculated from the geometries observed in the solid state. Interestingly, the values matched well with those obtained from the solid state conformation (**C1** conformation for compounds **2** and **4**, and **C2** conformation for **3**, see Figure S2). In its experimental geometry, **5** has one aryl group displaying a conformation very close to **C2** (leading to very similar $V_{s,max}$ values), whereas the second aryl has a conformation in between **C1** and **C2**.

Table 1. V_{max} values (kJ.mol⁻¹) on $\rho=0.001$ a.u. isosurface for the two most stable conformations of diaryl ditellurides **C1** and **C2** (σ_{Te-Te} denotes the σ -hole found in the prolongation of the Te-Te bond, whereas σ_{Te-C} refers to the one in the direction of C-Te bond).



Compound	Conformer 1 (C1)		Conformer 2 (C2)	
	σ_{Te-Te}	σ_{Te-C}	σ_{Te-Te}	σ_{Te-C}
1	48.9	35.9	76.3	40.7
2	36.2	31.1	65.6	36.2
2 (crystal)	34.5/33.6 ^[a]	22.1/22.9 ^[a]		
3	114.5	106.3	145.8	107.5
3 (crystal)			147.8	112.7
4	67.7	48.5	- ^[b]	60.6
4 (crystal)	65.6	44.6		
5	90.3	88.9	118.0	83.1
5 (crystal) ^[c]	105.6	83.3	115.4	80.0
6 ^[d]			71.8	36.5

[a] The two values correspond to the two crystallographic inequivalent Te atoms (Te1 and Te2 in Figure 4); [b] In this conformation a fluorine atom of the CF₃ group interacts with the σ_{Te-Te} . For **4** only the conformations with CF₃ groups oriented both toward the outside are reported; [c] For **5** (its crystal structure) one aryl displays a conformation very close to **C2** whereas the second one displays an intermediate conformation; [d] **C2** was the only stable conformation obtained by DFT calculations.

As expected, for compounds **1-3** and **5-6**, V_{max} is increasing with the electron-withdrawing ability of the R₁ substituent, whatever the considered conformation and σ -hole ($V_{max}(\mathbf{2}) < V_{max}(\mathbf{6}) < V_{max}(\mathbf{5}) < V_{max}(\mathbf{3})$). Nevertheless, a clear difference appeared in the σ -hole deepness; $V_{max}(\sigma_{Te-Te})$ values are always higher than $V_{max}(\sigma_{Te-C})$ with a larger difference in the case of **C2** conformation. This was unexpected since the Te-C bond is more polarized than the Te-Te bond.

In order to rationalize the observed relative order $V_{max}(\sigma_{Te-Te}) > V_{max}(\sigma_{Te-C})$ on diaryl ditellurides, additional calculations were performed on simple ditelluride model compounds HTeTeY, varying the Y substituent and using the same calculation conditions (Table 2 and SI, §4). In each case, the optimized structures resulted in H-Te-Te-Y dihedral angle close to 90°.

Moreover, in each case, two σ -holes were found on each Te atom (Figures 3 and S55-S56), one in the prolongation of Te-Te bond and the other in the prolongation of Te-H or Te-Y bond. Varying the Y substituent from EDG such as CH₃ to EWG such as CF₃ induced an increase in the Te Bader charge (from +0.20 to +0.27) and also a general increase of V_{max} at both σ -holes. In each case the σ -hole found in prolongation of Te-Te bond was found more electropositive than the one lying in the Te-Y direction.

Table 2. V_{max} values (kJ.mol⁻¹) on $\rho=0.001$ a.u. isosurface for HTeTeY model compounds

Compound	Conformer ^[b]	V_{max} (kJ.mol ⁻¹) ^[a]			
		$\sigma_{Te(\alpha)-H}$	$\sigma_{Te(\alpha)-Te(\beta)}$	$\sigma_{Te(\alpha)-Te(\beta)}$	$\sigma_{Te(\beta)-Y}$
HTeTeH ^[c]	-	66.0	97.7	97.7	66.0
HTeTeCH ₃	-	55.3	79.5	96.1	39.5
HTeTeCH ₂ F	A1	71.6	93.5	116.2	57.3
	A2	63.2	94.4	116.2	57.4
HTeTeCHF ₂	B1	71.1	103.2	145.0	72.6
	B2	84.7	110.0	84.9	77.5
	B3	77.9	110.5	84.0	77.5
HTeTeCF ₃	-	87.9	119.7	95.3	102.0

[a] The considered Te σ -hole is indicated in bold: Te(α) is linked to H and Te(β) is linked to Y; [b] See Figures 3, S55 and S56 for the positions of Te σ -holes; [c] Y = H, therefore Te(α) and Te(β) are equivalent.

For these model ditellurides, Natural Bond Orbital (NBO) analysis of the donor – acceptor interaction was performed on each optimized structure using the NBO 6.0 software^[29] (Table S12). This analysis shows that a significant stabilization occurs between one Te lone pair and the antibonding $\sigma^*(Te-H,Y)$ of the adjacent Te atom (Figure 2). Besides explaining the almost perpendicular geometry of (TeH)₂, i.e. a *gauche* effect, this stabilizing hyperconjugation contribution^[30] also induces a less electropositive σ -hole in the direction of Te-H by populating the $\sigma^*(Te-H)$ antibonding (the population of $\sigma^*(Te-H)$ antibonding is 0.026, larger than the population found for $\sigma^*(Te-Te)$ antibonding (0.003 for example in the case of H-Te-Te-H). In the anti-periplanar conformation, for which the Te lone pair to $\sigma^*(Te-H)$ stabilization is not possible due to unfavorable overlap, the two Te σ -holes are much more similar (e.g. for H-Te-Te-H: $V_{max}=111.4$ and 95.1 kJ.mol⁻¹ for σ -hole(Te-Te) and σ -hole(Te-H), respectively). Similar results were obtained on the whole HTeTeY series indicating that hyperconjugation contribution to tellurium σ -hole along Te-C bond can be generalized to substituted ditellurides, including diaryl ditellurides.

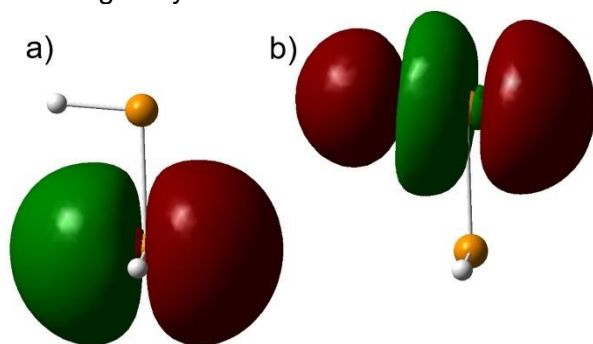


Figure 2. Donor-acceptor interactions NBO analysis in H-Te-Te-H model compound. The a) Te lone pair orbital favourably overlaps with b) the antibonding $\sigma^*(Te-H)$ giving rise to a stabilizing hyperconjugation (*gauche*) effect.

The V value at a given point of space does not depend only on the local electron density but is also affected by neighboring atoms, especially if they carry net charges. V values are thus conformation dependent. This is illustrated with HTeTeCHF_2 having 3 possible conformations (Figure 3). Indeed, $\text{Te}(\beta)$ σ -hole in prolongation of Te-Te bond is strongly electrophilic ($145.0 \text{ kJ}\cdot\text{mol}^{-1}$) when C-H bond is oriented parallel to Te-Te bond (conformation **B1**), bringing the electropositive H atom ($q(\text{H})=+0.06|e|$) in the vicinity of the σ -hole. Conformations **B2** and **B3**, where one of the two C-F bonds approaches the strongly electronegative fluorine atoms ($q(\text{F})=-0.62|e|$) toward the $\text{Te}(\beta)$ σ -hole position, induce a lowering of the strength of this σ -hole (down to $\sim 84.4 \text{ kJ}\cdot\text{mol}^{-1}$). It is worth noting that the other σ -holes are much less sensitive to CHF_2 conformations. The charge contribution is probably less important in the case of 3,5-disubstituted diaryl ditellurides when the charged substituents are placed far enough from Te σ -holes, whatever the conformation induced by aryl rotation along Te-C bond (e.g. in **3** the *ortho*-H atom is almost neutral with $q(\text{H})=+0.04|e|$; Figure S4). However, for compound **4**, one reason for the observed much lower V_{max} values of tellurium σ -holes compared to **3** could be due to charge contribution from the *ortho*- CF_3 group.

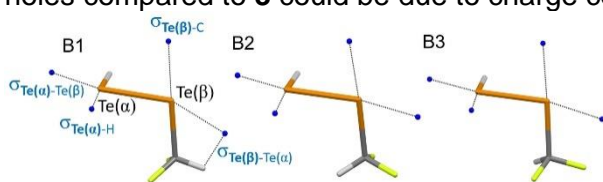


Figure 3 Positions of ESP maxima corresponding to Te σ -holes in the three conformations of HTeTeCHF_2 model molecule, shown as small blue spheres. Black dashed lines relate these σ -holes to neighbouring atoms.

The ability of compounds **2-4** to be involved in σ -hole based noncovalent interactions was first investigated in the solid-state.

The tellurium atom seems to play a central role in the crystal structure of **2**. For this compound, the crystal structure consists of infinite chains oriented along $[101]$ direction, where adjacent molecules interact through $\pi\cdots\pi$ stacking (inter-plane distance = $3.346 / 3.295 \text{ \AA}$) (Table S8, entries 1 and 2) and weak $\text{CH}\cdots\text{O}$ hydrogen bonds involving the four methoxy oxygen atoms ($d(\text{H}\cdots\text{O})=2.53\text{-}2.64 \text{ \AA}$) (Figure S14) and forming $\text{R}_2^2(7)$ motifs.^[31] Adjacent $[101]$ chains interact mainly through $\text{Te}\cdots\text{Te}$ intermolecular bonds (see below and Table S8, entry 4), forming (010) infinite planes. These planes then stack along $[010]$ direction, interacting mainly through $\text{Te}\cdots\text{C}_{\text{Ar}}$ ($\text{Te}2\cdots\text{C}6=3.629 \text{ \AA}$, $\text{RR}=0.97$, $\text{Te}1\text{-Te}2\cdots\text{C}6=175.5^\circ$) (Table S8, entry 3). The major remarkable chalcogen interaction here lead to the formation of a cyclic planar quadrangular Te_4 motif centered on an inversion center (Figures 4 and S17), where the tellurium σ -hole in the prolongation of $\text{C}_{\text{Ar}}\text{-Te}$ bonds interacts with one lone pair of the neighboring Te atom ($\text{Te}1\cdots\text{Te}2 = 3.918 \text{ \AA}$, $\text{RR}=0.95$) in a nearly linear geometry ($\text{C}1\text{-Te}1\cdots\text{Te}2 = 168.42^\circ$).

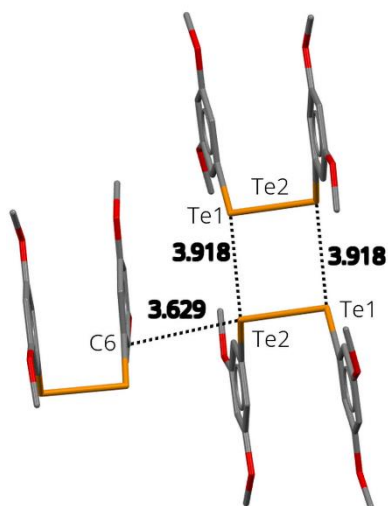


Figure 4. Chalcogen interactions in the crystal structure of **2**, shown as black dashed lines and forming a cyclic planar quadrangular Te₄ motif. Hydrogen atom omitted for clarity. Representative distances are given in Å

Such chalcogen interactions are also involved in the stabilization of the crystal structure of **5**. Indeed, the most stabilizing interaction (Table S11 entry 1), resulting in the formation of infinite chains along [010] direction, consists of ChB with one aromatic ring as the acceptor (Te₂...C8=3.569 Å, RR=0.95, Te₁-Te₂...C8=156.7°), completed with favorable dispersive contribution arising from aromatic ring proximity (Figure S34). These columns are then held together through secondary interactions. The most stabilizing one (Table S11, entry 2) involves also chalcogen interactions (Figure 5), forming a triangular Te₃ motif. In this molecular arrangement the σ-hole of Te₂ atom of a given molecule points toward a lone pair of Te₂ atom of the neighboring molecule (Te₂...Te₂=4.103 Å, RR=1.00, C7-Te₂...Te₂=149.44°) whereas one of its own lone pair acts as a ChB acceptor through its interaction with the σ-hole of Te₁ atom (Te₁...Te₂=3.945 Å, RR=0.96, C1-Te₁...Te₂=173.36°). These two contacts are somewhat frustrated, due to the interplay of the other interactions. Indeed, the first one deviates from linearity (even if σ-holes are not always located exactly in the direction of the prolongation of the covalent bond that creates them, the angle between Te₂...V_{S,max} and Te₂...Te₂ directions is 30.78°) and in the second one the angle between the Te₂ atom and the V_{S,min} point corresponding to the lone pair directions and the same Te₂ atom to neighboring Te₁ is 34.37° (Figure S53). The formation of these ChBs is confirmed by the observation of bond critical points (Figure S54) in the topological analysis of the DFT calculated electron density; the delocalization index, which can be seen as a measure of a bond degree is non negligible (~0.1), amounting about 10% of the corresponding value for the covalent C-Te bond itself.

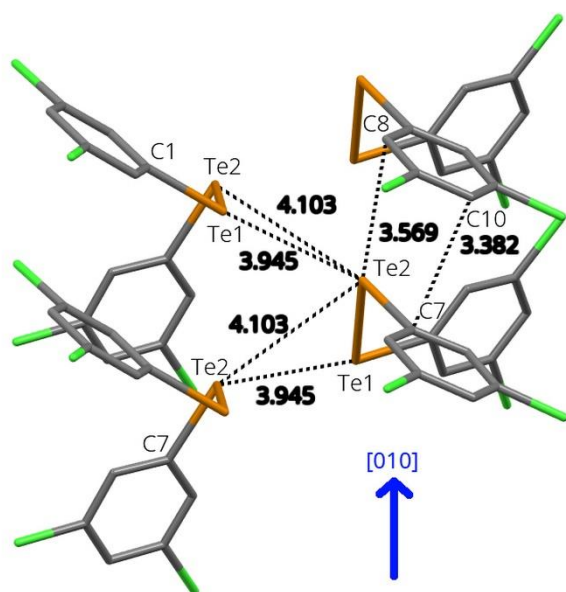


Figure 5. Triangular Te_3 motif built by chalcogen interactions in the crystal structure of **5**, shown as black dashed lines. Representative distances are given in Å. Hydrogen atoms are omitted for clarity.

A CSD search of the quadrangular and triangular motifs in diaryl ditellurides was performed (Table S3). It outputs only eight and twelve structures displaying respectively the triangular and quadrangular molecular arrangements, with $\text{Te}\cdots\text{Te}$ distances ranging from 3.769 to 4.168 Å. It is worth noticing that the interaction energy calculated for the Te_4 motif in **2** (-28 kJ/mol; Table S8, entry 4) is in line with the energies previously calculated on series of model chalcogen molecules (-14 – -25 kJ/mol).^[32] Although relatively weak, such ChB underlines the structure directing ability of these interactions in the solid state, in which a dispersion contribution has a significant role.

To better understand these structures, enrichment ratios (E)^[33] were computed for compounds **2-5** by comparing the actual surface contacts to equiprobable contacts based on the Hirshfeld surface. The obtained results (Tables S4-S7) show that these compounds adopt different molecular packing. Whereas **2** and **4** show enriched aromatic $\text{C}_{\text{Ar}}\cdots\text{C}_{\text{Ar}}$ contacts ($E=1.93$ and $E=2.29$) associated with $\pi\cdots\pi$ stacking, compound **3** displays impoverished $\text{C}_{\text{Ar}}\cdots\text{C}_{\text{Ar}}$ contacts ($E=0.84$). The similarity between **2** and **4** is reinforced considering that both structures display enriched $\text{Te}\cdots\text{Te}$ contacts ($E=1.35$ and $E=1.47$, respectively) whereas these contacts are clearly impoverished in **3** ($E=0.34$). In this latter structure, the tellurium atoms experience enriched contacts to aromatic rings ($E=2.1$), such contacts being slightly impoverished in **2** and **4** ($E=0.96$ and $E=0.82$, respectively). Compound **5** shows a strong enrichment of $\text{Te}\cdots\text{Te}$ contacts ($E=2.44$), corresponding to the formation of the Te_3 motif (see above). Whereas $\text{Te}\cdots\text{Cl}$ contacts are impoverished ($E=0.44$), numerous contacts appear between hydrogen atoms and chlorine and aromatic carbon (respectively $E=1.38$ and 1.22), corresponding to weak hydrogen interactions (Figures S36 and S37).

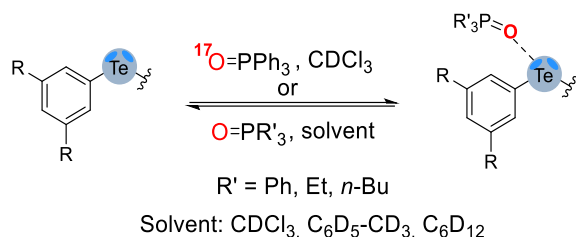
The full structural analysis (see SI, §2.3) prove that chalcogen atoms, even if they are not always engaged in contacts shorter than the van der Waals limit, are actively participating in favorable intermolecular interactions with neighboring molecules, thus contributing to the overall stabilization of the structures.

As expected, XRD structures of the diaryl ditellurides **2-5** revealed the presence of several noncovalent interactions, especially $\text{Te}\cdots\text{Te}$ and $\text{Te}\cdots\pi$ chalcogen bonds, but are they maintained in solution?

To look for such interactions in solution, we studied derivatives **1-6** through NMR spectroscopy. Looking at ^{125}Te nucleus can be advantageous to study noncovalent interactions involving tellurium and useful to quantify the effect of Te substituents. Because ^{125}Te NMR is

known to be sensitive to Te chemical environment,^[34] we expect ¹²⁵Te NMR chemical shifts to be influenced by both noncovalent interactions involving Te atoms, despite their weakness,^[16] and substituent effect.

To specifically probe noncovalent interactions involved in ChB, we first submitted each diaryl ditelluride **1-6** to a stoichiometric amount of triphenylphosphine oxide (Ph₃PO) in deuterated chloroform and monitored the resulting modifications by NMR (Scheme 3 and Table S13). Indeed, this Lewis base has already proven its efficiency as σ -hole acceptor in XB experiments^[35] and was recently used by our group for ChB detection.^[11e] Noticeably, Ph₃PO was ¹⁷O-enriched with the objective to monitor ¹⁷O chemical shift variation ($\Delta\delta$) together with ³¹P $\Delta\delta$, by ¹⁷O and ³¹P NMR spectroscopies, owing to the high sensitivity of these nuclei.



Scheme 3. ¹²⁵Te, ¹⁷O and ³¹P NMR monitoring of the interaction between diaryl ditellurides **1-6** and phosphine oxides.

Despite the weakness of the interaction, chemical shift variations up to 0.91 and 0.18 ppm were obtained, respectively in ¹⁷O and ¹²⁵Te NMR. These variations probably reflect the direct interactions between the ditelluride tellurium atom and the oxygen atom of the Lewis base. Lower variations were observed with ³¹P ($\Delta\delta = 0.04$ - 0.09 ppm), as expected from secondary interaction with the Lewis base phosphorous atom. Furthermore, a good correlation could be established between $\Delta\delta(^{125}\text{Te})$ and $\Delta\delta(^{17}\text{O})$ with the σ_{meta} Hammett parameters of the R substituents in compounds **1-3** and **5-6** (Figures 6 and S57). A direct link between the electronic effect of the aryl *meta* substituent and the tellurium σ -hole could thus be established, in line with ESP values. These set of data supported the presence of Te...O interaction in solution, even in a polar and possibly competitive solvent.

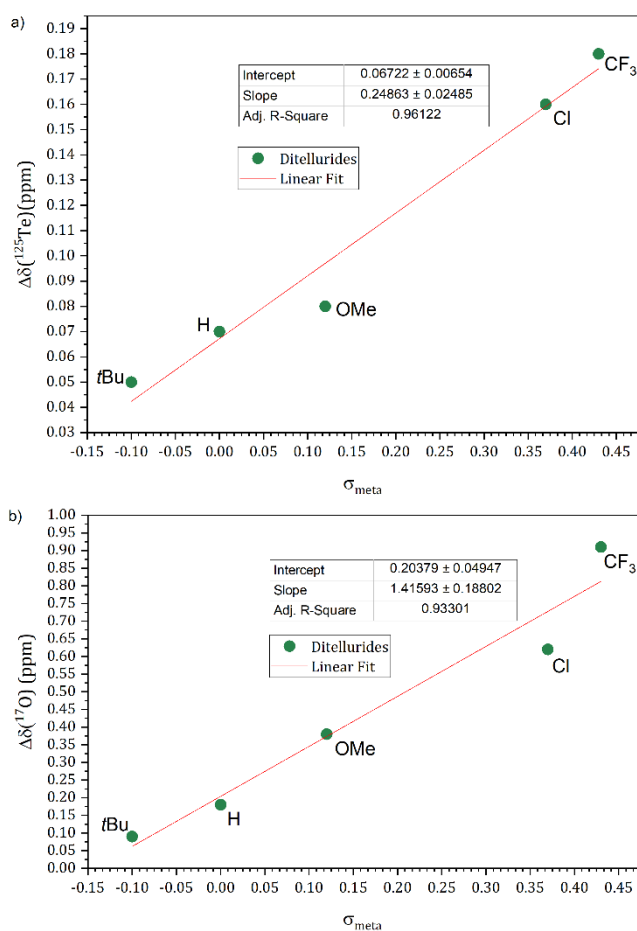


Figure 6. Linear regression analysis describing the relationships between $\Delta\delta(^{125}\text{Te})$ and σ_{meta} (a) and between $\Delta\delta(^{17}\text{O})$ and σ_{meta} (b).

It is worth noting that the *ortho*-substituted compound **4** exhibited weak to extremely weak chemical shift variations ($\Delta\delta$ 0.02 to 0.12 ppm) despite the strong electron-withdrawing nature of the σ -CF₃ group. Such low effect of adding Lewis base is in line with ESP data (Table 1) and suggests that the strong intermolecular π - π , electrostatic and Te \cdots Te interactions observed in the solid state for this compound (see SI, §2.3) are probably also active in solution. Indeed, intramolecular interaction between a CF₃ fluorine atom and Te σ -hole cannot be ruled out in solution, due to the rather short Te \cdots F distance (Te \cdots F = 3.31-3.38 Å, Figures S2 and S31). Both interaction types would thus minimize the formation of complex with the added Ph₃PO Lewis base.

As we recently demonstrated that chlorinated solvents clearly interact in solution with Te σ -holes,^[12] we performed similar experiments with less competitive solvents than CDCl₃, i.e. toluene-*d*8 and cyclohexane-*d*12. In order to increase the strength of the Te \cdots O interaction, a stronger σ -hole acceptor (Et₃PO^[36]) was also used. Under such conditions, NMR titration experiments could be performed, while titrations in CDCl₃ were not conclusive.^[37] From the so-obtained data, association constants (K_a) could be obtained and compared (Table 3). NMR titration indeed provides an established tool for characterizing the strength of supramolecular adducts, in particular by giving access to their association constants and stoichiometry.^[38] Diaryl ditellurides **1** and **3**, whose concentrations were kept constant, were mixed in a deuterated solvent with increasing concentrations of phosphine oxide, while ¹²⁵Te NMR spectra were collected (see SI, §5.2).

As expected from ESP data, whatever the phosphine oxide/solvent system, higher values of K_a were obtained for ditelluride **3** bearing EWG (entries 1 vs 2 and 3 vs 4). Shifting the Lewis base from Ph₃PO to Et₃PO only induced a slight change in deuterated toluene (entries 1 vs 3,

and 2 vs 4). As small Te... π interactions were observed in the solid state (see Figure S3), toluene might not be a not-so-innocent solvent, we shifted to an even less interacting solvent, cyclohexane, expecting to observe stronger Te...Lewis base interactions. Rewardingly, NMR titration experiments in deuterated cyclohexane led to an important K_a increase (entries 5 vs 4 vs 2). Such large K_a increases (15-times) clearly reflect the stronger interaction which can be achieved with stronger σ -hole acceptors in less and less interacting solvents.

Table 3. Experimental K_a values of the ArTeTeAr...OPR₃ adducts^[a]

Entry	ArTeTeAr (R)	OPR ₃	Solvent	K_a (M ⁻¹) ^[b]
1	1 (R = H)	OPPh ₃	Toluene- <i>d</i> 8	0.23 ± 0.01
2	3 (R = CF ₃)	OPPh ₃	Toluene- <i>d</i> 8	5.70 ± 0.20
3	1 (R = H)	OPEt ₃	Toluene- <i>d</i> 8	0.26 ± 0.03
4	3 (R = CF ₃)	OPEt ₃	Toluene- <i>d</i> 8	5.90 ± 0.20
5	3 (R = CF ₃)	OPEt ₃	Cyclohexane- <i>d</i> 12	91.00 ± 9.00

[a] Conditions: The initial concentration of ArTeTeAr is 20 mM (see SI, §5.2 for details); [b] Determined from non-linear regression modelling of 1:1 binding isotherm collected during NMR titrations.

The mixture of **3** and Et₃PO in cyclohexane showing the highest value of K_a (Table 3, entry 5) was then considered in order to detect the Te...O interaction by 2D NMR. We wondered if ¹⁹F-¹H HOESY could be used to trace the putative spatial proximity of Et₃PO hydrogens with ditelluride fluorines in **3**/Et₃PO adduct.^[39] Unfortunately, the HOESY spectrum of the mixture composed of ditelluride **3** and 10 equivalents of Et₃PO in cyclohexane-*d*12 did not show any cross-peak that could be assigned to H-F spatial proximity. Pleasingly, by using *n*Bu₃PO with longer alkyl arms, cross-peaks involving CH₂-CH₃ and CF₃ fragments were observed, confirming the adduct formation in solution (Figures 7 and S63).

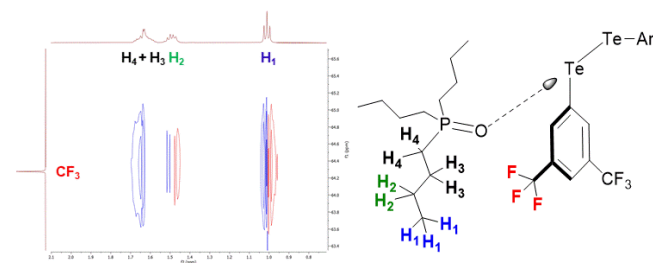


Figure 7. ¹⁹F-¹H HOESY NMR spectrum of a mixture of **3** (20 mM) with Bu₃PO (196 mM) in cyclohexane-*d*12.

Overall, these results show that ArTeTeAr•OPR₃ adducts could be formed in solution and that the aryl substituents play key role in establishing ChB. As expected, adjusting the electronic nature of the Te substituent clearly allows to tune the ChB strength by acting on the Te σ -hole deepness.

Conclusion

We reported here the synthesis and the study of σ -hole properties of differently substituted diaryl ditellurides, in solution and in solid-state. Of the two Te σ -holes, the one at the opposite of the Te-Te bond was found to be more electropositive compared to the one at the opposite of the Te-C_{Ar} bond. This unexpected result could be rationalized by NBO analysis evidencing the hyperconjugation contribution from one Te lone pair to the σ^* of the adjacent Te atom resulting in electronic enrichment of the σ -hole at the opposite of the more polarized Te-C_{Ar} bond.

The crystal structure analysis of four representative diaryl ditellurides showed that Te σ -hole interactions are involved in the crystal packing. In particular, one derivative forms a Te₄ rectangle structure through dimerization via intermolecular Te...Te ChB. Another compound forms a triangular Te₃ motif, where one chalcogen interacts with both Te atoms of a neighboring molecule through both its σ -hole and its lone pair, in a slightly frustrated geometry. ChB involving π acceptors are also clearly evidenced, and in the other investigated structures, even if directional contacts are less strong, a clear interaction scheme involving Te σ -holes appears, underlying the importance of these secondary interactions.

Weak interactions with OPPh₃ could be identified in chloroform by combining multinuclear NMR, especially ¹²⁵Te and ¹⁷O NMR. Interestingly, stronger interactions were evidenced by using the more Lewis basic OPET₃ and less- and non-interacting solvents such as toluene and cyclohexane. With diaryl ditelluride bearing CF₃ groups, association constants $K_a \geq 1$ could be measured for the 1:1 adducts by titration experiments in ¹²⁵Te NMR. The highest value of $K_a = 90 \text{ M}^{-1}$ was measured in cyclohexane. Moreover, by using *n*Bu₃PO as the Lewis base, the ¹⁹F-¹H HOESY experiment showed spatial proximity between CF₃ and CH₃ of *n*Bu₃PO, definitively proving that Te...O interaction occurred in solution.

Experimental Section

General procedure for the synthesis of diaryl ditellurides 2-6. A 1.7 M solution *t*-butyllithium in pentane (2.1 eq.) was added dropwise to haloarene (1 mmol, 1 eq.) in freshly distilled THF (10 mL) at -78 °C, under argon. The mixture was stirred for 1 h at -78 °C (color changes from pale yellow to orange/brown). Then tellurium powder (1.7 mmol, 1.7 eq) was added in one portion, the cooling bath was removed and stirring was continued for 5 h at rt (color changes to dark red). Then the reaction mixture was quenched by pouring it into an Erlenmeyer flask equipped with a magnetic stirring bar (rod) containing water cooled with ice (25 mL). The resulting black solution was stirred overnight under air. The mixture was filtered at vacuum over a 4 cm thick Celite pad placed in a fritted glass (porosity 1, diameter 6 cm). The pad was washed with CH₂Cl₂ (3 x 40 mL). Phases were separated and the aqueous phase was extracted with CH₂Cl₂ (40 mL). Organic extracts were combined, shortly dried over MgSO₄, filtered and concentrated. Purification was achieved by chromatography on a silica gel column using a pentane / CH₂Cl₂ gradient from 10:0 to 6:4, or pure pentane with apolar compounds.

NMR Titration experiments. For pipetting Hamilton®-syringes were used. All experiments were conducted at ambient temperature (298.5 K) and in NMR tubes. For each sample, a set amount of the ChB donor was weighted on an analytical balance into a Volumetric flask and a specific amount of the ChB acceptor was also weighted in another one. They were subsequently diluted carefully in the volumetric flask to volume with the corresponding solvent of titration. Each mixture was then agitated for at least 5 min to fully dissolve all solids and mix the solution thoroughly prior to transferring to NMR tubes. Each titration experiment involves at least nine sequential samples, in which the concentration of the ChB donor is kept constant (0.02 M, 0.45 mL before dilution), whereas the concentration of the ChB acceptor is systematically increased from 0.0 M up to 1.0 M (depending on the donor-acceptor-solvent system). The NMR tube was manually agitated 5 min before the acquisition of ¹²⁵Te. ¹H NMR was systematically recorded to check the homogeneity of the solution in the tube. Throughout each titration experiment all parameters of the NMR spectrometer remained constant. The measured shifts were plotted against the guest-equivalents and the resulting curve was fitted using <http://supramolecular.org/>. For the calculation of the binding constants (K), a 1:1 binding was assumed.

X-Ray Diffraction. Single crystals of **2-5** suitable for the single X-ray analysis were obtained from slow evaporation of their corresponding solution in acetone, in absence of light. The crystals of **2-5** were placed in oil, and a single crystal was selected, mounted on a glass fiber and placed in a low-temperature N₂ stream. X-ray diffraction data collection was carried out on

a Bruker PHOTON III DUO CPAD diffractometer equipped with an Oxford Cryosystem liquid N₂ device, using Mo-K α radiation ($\lambda = 0.71073 \text{ \AA}$). The crystal-detector distance was 37 mm. The cell parameters were determined (APEX3 software)^[40] from reflections taken from 1 set of 180 frames at 1s exposure. The structures were solved using the program SHELXT-2014.^[41] The H-atoms were included in calculated positions and treated as riding atoms using SHELXL default parameters. The non-H atoms were refined anisotropically, using weighted full-matrix least-squares on F². A semi-empirical absorption correction was applied using SADABS in APEX3; transmission factors: $T_{\min}/T_{\max} = 0.6765/0.7463$ for **2**; $T_{\min}/T_{\max} = 0.6981/0.7456$ for **4**; $T_{\min}/T_{\max} = 0.5242/0.7456$ for **3**; $T_{\min}/T_{\max} = 0.5932/0.7458$ for **5**. In the latter case, the structure was refined as a 2-component inversion twin, with a ratio of 0.48/0.52 for the two domains. Deposition Number(s) 2081477 (for **2**), 2081476 (for **3**), and 2081475 (for **4**), and 2144457 (for **5**) contain(s) the supplementary crystallographic data for this paper. These data are provided by the joint Cambridge Crystallographic Data Centre and Fachinformationszentrum Karlsruhe Access Structures service www.ccdc.cam.ac.uk/structures.

In order to rationalize the crystal structures, intermolecular interaction energies were calculated with CrystalExplorer^[42] (details in SI, §2.5).

DFT calculations. Molecular geometries of compounds **2-4** were extracted from the corresponding experimental X-ray structures. Hydrogen atom positions were optimized (while keeping the other atoms fixed) at the DFT level of theory (B3LYP functional completed with D3 dispersion correction;^[27] Def2TZVPP basis set) using the Gaussian09 software.^[43] Isosurface of electron density ($\rho=0.001 \text{ a.u.}$) mapped with the corresponding total electrostatic potential were calculated and drawn with AIMAll software;^[44] characterization of $V_{S,\max}$ extrema of the EP was performed MultiWfn programs.^[28]

Acknowledgements

This research was funded by the International Center Frontier Research in Chemistry (icFRC), the LabEx CSC (ANR-10-LABX-0026 CSC) and French National Research Agency (ANR-21-CE07-0014). RB thanks the LabEx CSC, Strasbourg, for a PhD fellowship. LG thanks the ANR for a PhD fellowship. The EXPLOR mesocenter is thanked for providing access to their computing facility (project 2019CPMXX0984/wbg13).

Keywords: chalcogen bond • diaryl ditelluride • σ -hole • supramolecular interaction • ¹²⁵Te NMR

- [1] a) J. Bamberger, F. Ostler, O. G. Mancheño, *ChemCatChem* **2019**, *11*, 5198-5211; b) R. L. Sutar, S. M. Huber, *ACS Catal.* **2019**, *9*, 9622-9639; c) M. Breugst, J. J. Koenig, *Eur. J. Org. Chem.* **2020**, 5473-5487.
- [2] a) P. Auffinger, F. A. Hays, E. Westhof, P. S. Ho, *PNAS* **2004**, *101*, 16789-16794; b) R. Wilcken, M. O. Zimmermann, A. Lange, A. C. Joerger, F. M. Boeckler, *J. Med. Chem.* **2013**, *56*, 1363-1388.
- [3] A. Mukherjee, S. Tothadi, G. R. Desiraju, *Acc. Chem. Res.* **2014**, *47*, 2514-2524.
- [4] a) S. Kolb, G. A. Oliver, D. B. Werz, *Angew. Chem. Int. Ed.* **2020**, *59*, 22306-22310; b) S. Kolb, G. A. Oliver, D. B. Werz, *Angew. Chem.* **2020**, *132*, 22490-22495.
- [5] a) L. Vogel, P. Wonner, S. M. Huber, *Angew. Chem. Int. Ed.* **2019**, *58*, 1880-1891; b) N. Biot, D. Bonifazi, *Coord. Chem. Rev.* **2020**, *413*, 213243.
- [6] C. B. Aakeroy, D. L. Bryce, G. R. Desiraju, A. Frontera, A. C. Legon, F. Nicotra, K. Rissanen, S. Scheiner, G. Terraneo, P. Metrangolo, G. Resnati, *Pure Appl. Chem.* **2019**, *91*, 1889-1892.
- [7] a) J. S. Murray, P. Lane, T. Clark, P. Politzer, *J Mol Model* **2007**, *13*, 1033-1038; b) T. Clark, *Faraday Discuss.* **2017**, *203*, 9-27.
- [8] R. Gleiter, G. Haberhauer, D. B. Werz, F. Rominger, C. Bleiholder, *Chem. Rev.* **2018**, *118*, 2010-2041.
- [9] H. Zhao, F. P. Gabbaï, *Nat. Chem.* **2010**, *11*, 984-990.
- [10] a) G. E. Garrett, G. L. Gibson, R. N. Straus, D. S. Seferos, M. S. Taylor, *J. Am. Chem. Soc.* **2015**, *137*, 4126-4133; b) L. M. Lee, M. Tsemperouli, A. I. Poblador-Bahamonde, S. Benz, N. Sakai, K. Sugihara, S. Matile, *J. Am. Chem. Soc.* **2019**, *141*, 810-814; c) B. Zhou, F. P. Gabbaï, *Chem. Sci.* **2020**, *11*, 7495-7500.
- [11] a) S. Benz, A. I. Poblador-Bahamonde, N. Low-Ders, S. Matile, *Angew. Chem. Int. Ed.* **2018**, *57*, 5408-5412; *Angew. Chem.* **2018**, *130*, 5506-5510; b) P. Wonner, A. Dreger, L. Vogel, E. Engelage, S. M. Huber, *Angew. Chem. Int. Ed.* **2019**, *58*, 16923-16927; *Angew. Chem.* **2019**, *131*, 17079-17083; c) P. Wonner, T. Steinke, L. Vogel, S. M. Huber, *Chem. Eur. J.* **2020**, *26*, 1258-1262; d) T. Steinke, P. Wonner, E. Engelage, S. M. Huber, *Synthesis* **2021**, 53, 2043-2050; e) R. Weiss, E. Aubert, P. Pale, V. Mamane, *Angew. Chem. Int. Ed.* **2021**, *60*, 19281-19286; f) B. Zhou, F. Gabbai, *J. Am. Chem. Soc.* **2021**, *143*, 8625-8630; g) B. Zhou, F. Gabbai,

- Organometallics* **2021**, *40*, 2371-2374; h) For a recent review, see: A. Frontera, A. Bauza, *Int. J. Mol. Sci.* **2021**, *22*, 12550.
- [12] R. Weiss, Y. Cornaton, H. Khartabil, L. Gros Lambert, E. Hénon, P. Pale, J.-P. Djukic, *ChemPlusChem* **2022**, 10.1002/cplu.202100518.
- [13] a) D. B. Werz, R. Gleiter, F. Rominger, *Organometallics* **2003**, *22*, 843-849; b) M. Rodewald, J. M. Rautiainen, T. Niksch, H. Görls, R. Oilunkaniemi, W. Weigand, R. S. Laitinen, *Chem. Eur. J.* **2020**, *26*, 13806-13818.
- [14] T. Shimizu, H. Isono, M. Yasui, F. Iwasaki, N. Kamigata, *Org. Lett.* **2001**, *3*, 3639-3641.
- [15] R. Oilunkaniemi, R. S. Laitinen, M. Ahlgrén, *Zeitschrift für Naturforschung B* **2000**, *55*, 361-368.
- [16] P. J. W. Elder, I. Vargas-Baca, *Phys. Chem. Chem. Phys.* **2016**, *18*, 30740-30747.
- [17] L. A. Ba, M. Döring, V. Jamier, C. Jacob, *Org. Biomol. Chem.* **2010**, *8*, 4203-4216.
- [18] M. Ibrahim, W. Hassan, D. F. Meinerz, M. dos Santos, C. V. Klimaczewski, A. M. Deobald, M. S. Costa, C. W. Nogueira, N. B. V. Barbosa, J. B. T. Rocha, *Mol. Cell. Biochem.* **2012**, *371*, 97-104.
- [19] a) C.-M. Andersson, A. Hallberg, R. Brattsand, I. A. Cotgreave, L. Engman, J. Persson, *Bioorg. Med. Chem. Lett.* **1993**, *3*, 2553-2558; b) L. Engman, D. Stern, M. Pelcman, C. M. Andersson, *J. Org. Chem.* **1994**, *59*, 1973-1979.
- [20] H. Sies, *Free Radical Biol. Med.* **1993**, *14*, 313-323.
- [21] A. Daolio, P. Scilabra, M. E. Di Pietro, C. Resnati, K. Rissanen, G. Resnati, *New J. Chem.* **2020**, *44*, 20697-20703.
- [22] The role of halogen bonds in medicinal chemistry is more documented, see: a) R. Wilcken, M. O. Zimmermann, A. Lange, A. C. Joerger, F. M. Boeckler, *J. Med. Chem.* **2013**, *56*, 1363-1388; b) A. Dessi, P. Peluso, R. Dallochio, R. Weiss, G. Andreotti, M. Allocca, E. Aubert, P. Pale, V. Mamane, S. Cossu, *Molecules* **2020**, *25*, 2212.
- [23] N. Petraghani, H. A. Stefani, *Tellurium in Organic Synthesis*, 2nd Ed., Academic Press, London, **2007**.
- [24] R. T. Mehdi, D. Miller, T. A. Tahir, *Inorg. Chimica Acta* **1984**, *90*, 85-89.
- [25] Low quality crystals of compound **7** showing the tellurium oxide backbone could be obtained. See Supporting Information for more details.
- [26] K. Srivastava, S. Sharma, H. B. Singh, U. P. Singh, R. J. Butcher, *Chem. Commun.* **2010**, *46*, 1130-1132.
- [27] S. Grimme, J. Antony, S. Ehrlich, H. Krieg, *J. Chem. Phys.* **2010**, *132*, 154104.
- [28] a) T. Lu, F. Chen, *J. Comput. Chem.* **2012**, *33*, 580-592; b) T. Lu, F. Chen, *J. Mol. Graph. Model.* **2012**, *38*, 314-323.
- [29] NBO 6.0. E. D. Glendening, J. K. Badenhoop, A. E. Reed, J. E. Carpenter, J. A. Bohmann, C. M. Morales, C. R. Landis, and F. Weinhold (Theoretical Chemistry Institute, University of Wisconsin, Madison, WI, 2013); <http://nbo6.chem.wisc.edu/>
- [30] U. Salzner, P. v. R. Schleyer, *J. Am. Chem. Soc.* **1993**, *115*, 10231-10236.
- [31] J. Bernstein, R. E. Davis, L. Shimon, N.-L. Chang, *Angew. Chem. Int. Ed. Engl.* **1995**, *34*, 1555-1573.
- [32] a) C. Bleiholder, D. B. Werz, H. Köppel, R. Gleiter, *J. Am. Chem. Soc.* **2006**, *128*, 2666-2674; b) C. Bleiholder, R. Gleiter, D. B. Werz, H. Köppel, *Inorg. Chem.* **2007**, *46*, 2249-2260.
- [33] C. Jelsch, K. Ejsmont, L. Huder, *IUCrJ* **2014**, *1*, 119-128.
- [34] H. C. E. McFarlane, W. McFarlane, in *NMR of Newly Accessible Nuclei*. (Ed: P. Laszlo), Academic Press, New York, **1983**, p. 275.
- [35] a) Y. Xu, L. Champion, B. Gabidullin, D. L. Bryce, *Chem. Commun.* **2017**, *53*, 9930-9933; b) Y. Xu, B. Gabidullin, D. L. Bryce, *J. Phys. Chem. A* **2019**, *123*, 6194-6209; c) A. S. Ostras', D. M. Ivanov, A. S. Novikov, P. M. Tolstoy, *Molecules* **2020**, *25*, 1406.
- [36] Y.-P. Chang, T. Tang, J. R. Jagannathan, N. Hirbawi, S. Sun, J. Brown, A. K. Franz, *Org. Lett.* **2020**, *22*, 6647-6652.
- [37] Chloroform could act as a competitor both for Te σ -holes (see ref 12), and for phosphine oxide through H-bond (We thank one referee for this suggestion).
- [38] P. Thordarson, *Chem. Soc. Rev.* **2011**, *40*, 1305-1323.
- [39] Q. M. Dang, J. H. Simpson, C.A. Parish, M. C. Leopold, *J. Phys. Chem. A* **2021**, *125*, 9377-9393.
- [40] Bruker (2012). APEX3. Bruker AXS Inc., Madison, Wisconsin, USA.
- [41] G. M. Sheldrick, *Acta Cryst.* **2015**, *A71*, 3-8.
- [42] M. J. Turner, J. J. McKinnon, S. K. Wolff, D. J. Grimwood, P. R. Spackman, D. Jayatilaka and M. A. Spackman, *CrystalExplorer17* (2017). University of Western Australia.
- [43] M. J. Frisch et al. *Gaussian 09* (Gaussian, Inc., Wallingford CT, 2009).
- [44] T. A. Keith, TK Gristmill Software, Overland Park KS, USA, AIMAll (Version 19.10.12), 2019 (aim.tkgristmill.com).